Electronic Journal of Structural Engineering

Original Article

Cite this: DOI:10.56748/ejse.24629

Received Date:01 May 2024
Accepted Date: 03 November 2024

1443-9255
https://ejsei.com/ejse

Assessment of Ductility Indices in FRP-Strengthened RC Beams: A Statistical Analysis

Diyaree Jalal Ghaidan[a b*], Ali Ihsan Salahaldin[b], Hasan Jasim Mohammed[a]
[a] Department of Civil Engineering, College of Engineering, University of Tikrit, Tikrit, Iraq
[b] Department of Civil Engineering, College of Engineering, University of Kirkuk, Kirkuk, Iraq
*Corresponding author: diyarij@uokirkuk.edu.iq

Abstract

The study aims to use statistical analyses to identify the optimal ductility indices that can characterize the behavior of FRP strengthened RC beams and assess the effects of the longitudinal reinforcements, expressed as total equivalent steel ratio (TESR%). The analyses are based on various techniques such as MANOVA, MANCOVA, and the Johnson-Neyman method. The results showed a significant relationship between TESR% and ductility indices at different levels of the moderator (stirrup ratio). The TESR% has a wide range of negligible regions on Naaman and Jeong's ductility index (0.74% to 1%) compared to Davies's and Oudah (0.72% to 0.87%) and El-Hacha's indexes (0.74% to 0.89%). Therefore, it appears that Naaman and Jeong's index may not provide an accurate assessment for RC beams strengthened by FRP material. The Oudah and El-Hacha index values are greater than those of other ductility indices due to the deformability ratio considered in the calculation. However, Davies's index was more sensible than the other two ductility indices due to its lower values.

Keywords

Ductility, Indices, MANOVA, MANCOVA, Johnson Neyman Method

1. Introduction

In recent years, researchers have become increasingly interested in using fiber-reinforced polymer (FRP) materials to enhance existing structures. This is mainly due to the many advantages these materials offer, such as their high strength-to-weight ratio, resistance to corrosion, and ease of installation. Although there has been a significant focus on strengthening RC structures with FRP, determining ductility for these components remains complex because of the unique characteristics of FRP materials and the potential for catastrophic failure (Salahaldin, Jomaa'h, and Naser 2021), (Salahaldin et al. 2022), (Oudah and El-Hacha 2012).

Structural ductility is an essential property for engineers as it redistributes the internal forces and the formation of plastic hinges prior to collapse under severe loading conditions. It is important to note that this property allows for a significant maximum warning prior to catastrophic failures, thereby avoiding sudden and catastrophic collapses under the limit state. The Conventional definition of ductility is based on the ratio of ultimate/yielding parameter elastic quantity, see Eq. (1) and Eq. (2). The descriptive indices of ductility are ultimate curvature (ψ_u) and yield curvature (ψ_y) as well as ultimate deflection (Δ_u) and yield deflection (Δ_y).

$$\mu_\psi = \frac{\psi_u}{\psi_y} \quad (1)$$

$$\mu_d = \frac{\Delta_u}{\Delta_y} \quad (2)$$

However, they are inadequate for FRP-strengthened beams (Spadea et al. 2015). Because there is no yielding point for RC strengthened with FRP due to the fundamental property of FRP materials as elastic materials, as shown in Fig.1, alternate methods for determining deformation capacity are required. To resolve this challenge, (Mufti, Newhook, and Tadros 1996) proposed a new term called "deformability" to quantify how a flexural behavior behaves in FRP strengthened beams. The alternative concept is based on the two cardinal points experienced by the FRP RC structures: the cracking point and the ultimate point. In addition, they also suggested using a deformability factor greater than 4.0 as a criterion for determining whether a structure has adequate warning signs before experiencing ultimate failure.

The Canadian Highway Bridge Design Code later adopted this index. To calculate this deformability factor (μ_M), as demonstrated in Eq. (3), several variables need consideration: M1 represents the maximum resisting moment at beam failure; ψ_u indicates the maximum curvature of the section; $M_{0.001}$ represents the resisting moment that corresponds to concrete compressive strain when it reaches 0.001; while $\psi_{0.001}$ stands for curvature at that specific level of compressive strain (0.001).

$$\mu_M = \left(\frac{\psi_u}{\psi_{0.001}}\right) * \left(\frac{M_u}{M_{0.001}}\right) \quad (3)$$

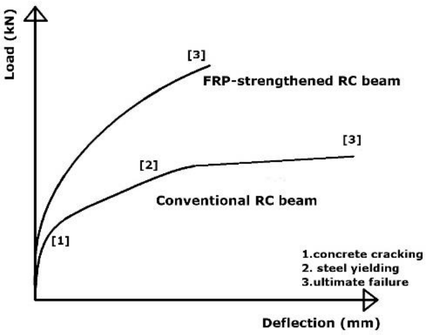

Fig. 1 Load–deflection curve (Davies 2010)

However, the amount of elastic energy released during failure is significantly higher in RC beams strengthened with FRP materials designed to fail due to FRP rupture. Therefore, a more realistic way to study the ductility of structural members would be to consider both the energy released by the specimen during failure and its deformation characteristics. According to (Naaman and Jeong 1995), a more representative approach for measuring ductility is based on the total energy and elastic energy just before failure, as denoted in Eq. (4).

$$\mu_N = 0.5\left(\frac{E_{tot}}{E_{ela}} + 1\right) \quad (4)$$

Calculating the area under the load-deflection curve up until the failure can determine the total energy or E_{tot}. On the other hand, E_{ela} represents the elastic stored energy in FRP-strengthened elements that is released upon failure. To estimate the value of E_{ela}, Eq. (5) can be used to predict the slope of the unloading curve, as shown in Fig. 2.

$$S_N = \frac{P_c S_1 + (P_y - P_c) S_2}{P_y} \quad (5)$$

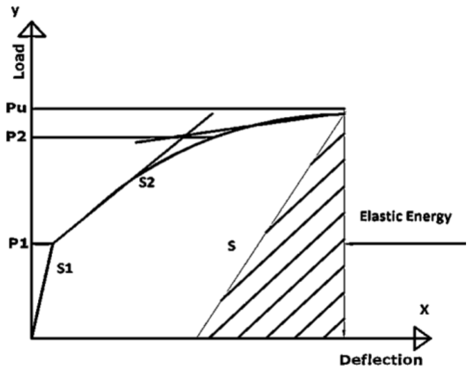

Fig. 2 Stored elastic energy at failure (Naaman and Jeong 1995)

However, (Davies 2010) study revealed that the underlying assumptions employed in developing this index are not suitable for predicting the behavior of FRP RC structures. These assumptions suggest that the structure performs elastically perfectly plastic and that the elastic energy stored within the system is equivalent to that of steel RC structures. Thereby, Davies proposed revising the Naaman and Jeong method by considering the additional elastic energy generated in any FRP-reinforced element during later stages of loading. This revised approach calculates the slope of the unloading curve using a third slope, S_3, referred to in Eq. (6) (see Fig. 3). The slope of the unloading branch is represented by S_N, while S_1 and S_2 represent the slopes of the first and second lines, respectively. P_c refers to a cracking load, whereas P_y denotes a yielding load. This index has been widely used in characterizing the ductility of RC structures strengthened with FRP materials and has been recommended by design guidelines ISIS Canada Design Manual 2008.

$$S_P = \frac{P_1S_1+(P_2-P_1)S_2+(P_U-P_2)S_3}{P_U} \quad (6)$$

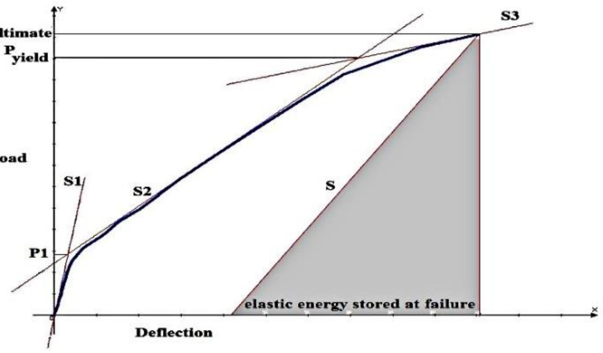

Fig. 3 Davies approach utilizing a third slope(S3) (Davies 2010)

Implementing this revised method allows for the determination of an adjusted value for estimated stored elastic energy, E_{ela}, which is employed to calculate the modified ductility index μ_P, as seen in Eq. (7).

$$\mu_P = 0.5\left(\frac{E_{tot}}{E_{ela}}+1\right) \quad (7)$$

Moreover, Oudah and El-Hacha [1], presented an innovative model for assessing both deformability and energy dissipation capacity in FRP-strengthening RC beams. They utilize trilinear load-deflection response and bilinear trend concepts to establish their model. The overall ductility can then be expressed by multiplying two factors: one being the ratio of deformability, while the other represents a compatibility factor, as denoted in Eqs. (8), (9), and (10).

$$\mu_O = \mu_d * \beta \quad (8)$$

$$\beta = \frac{S\Delta_y[P_y(\Delta_u-\Delta_c)+P_u(\Delta_u-\Delta_y)+P_c\Delta_y]}{P_u^2\Delta_u} \quad (9)$$

$$S = \frac{P_y-P_c}{\Delta_y-\Delta_c} \quad (10)$$

Although there is many available ductility indices used to examine the performance of RC beams strengthened with FRP materials, nonetheless, there is a significant lack of knowledge about many of these indices, which ones are more appropriate and which ones are not. The present study aims to address this issue and undertake the performance and limitations of ductility indices (Energy-based approach) for RC beams strengthened with FRP materials. This study will contribute significantly to the field of assessment beams strengthened with FRP materials by providing a statistically robust framework for selecting the most suitable ductility index. Additionally, the study examines the possibility of the effect of Total Equivalent Steel Ratio TESR% in calculating the ductility indices.

2. Research Methodology

2.1 Data of the RC beams strengthened with the FRP-NSM system

Table 1 presents a comprehensive summary of the geometric and material characteristics of the 99 specimens utilized in the published data. The key parameters highlighted in this table include the dimensions of the beam, such as width, height, span length, and shear span, as well as the concrete strength. Most of these samples had a width below 250 mm and a height ranging from 170 to 375 mm. The majority of beams had a span length of less than 4,000 mm and a shear span shorter than 1350 mm. The compressive strength of concrete (f_c') typically ranges from 20 MPa to 50 MPa. Moreover, it is often seen that the yield strength of reinforcing steels (f_y) normally ranges from 350 MPa to 600 MPa. Approximately 93% of the test programs utilized fiber-reinforced polymers (FRP) material with a tensile modulus (E_f) below 200 GPa, whereas the remaining 7% employed FRP with a high modulus. Most FRP materials exhibit a rupture strain ranging (E_u%) from 1.0% to 2.0%, which is considered standard for carbon fibre reinforced polymer (CFRP) composites. On the other hand, glass fiber reinforced polymer (GFRP), due to its lower modulus, tends to show higher rupture strains exceeding an εf_u value of 2.0%.

2.2 Data Analysis

The present study utilized a comparative research design to examine the data, employing the statistical program SPSS version 24. The statistical techniques of Multivariate Analysis of Variance (MANOVA) and Multivariate Analysis of Covariance (MANCOVA) were utilized, along with the Johnson-Neyman method. The ductility indices derived from the energy area ratios, at certain points (crack, yield, and ultimate) are displayed in Table 1. As mentioned in section 2.2, The calculation method was first presented by (Naaman and Jeong 1995). Additionally, two different methods were utilized to estimate the ductility: one revised method by (Davies 2010) and another suggested approach by (Oudah and El-Hacha 2012). In considering the evaluation of TESR, the assessment involves computing the overall area of the composite material and establishing an equivalent quantity of steel by applying Eq. (11), where 'αi' represents the modular ratio. The resulting Total Equivalent Steel Ratio is then represented as a proportion relative to the entire cross-sectional area, as demonstrated in Eq. (12).

$$\alpha_i = \frac{(E_{FRP})_i}{E_{Steel}} \quad (11)$$

$$TESR\% = \sum\frac{100(A_s+\alpha_i A_{FRP})}{bd} \quad (12)$$

Additionally, Table 1 provides information regarding both the stirrup ratio and the inclusion of anchorage in the FRP strengthening system. Several structural design codes define the stirrup ratio as follows:

$$\rho_{SV}\% = \frac{A_{SV}}{bs} \quad (13)$$

Where: A_{sv} is the total area of stirrups in the section of the beam, b is the beam width, and S is the stirrup spacing along the beam span.

Table 1. Summary of the experimental database

References	h mm	w mm	L mm	anchorage status	f_c'	f_y	E_f	E_u %	ρ_{SV} %	$TESR$ %	μ_N	μ_P	μ_O
(El-Hacha and Rizkalla 2004)	300	150	2700	Non-anch.	N/A	N/A	123	1.14	1.5	1.87	3.3	2.13	2.76
	300	150	2700	Non-anch.	N/A	N/A	140	1.08	1.5	1.87	3.07	1.97	2.38
	300	150	2700	Non-anch.	N/A	N/A	140	1.08	1.5	1.87	4.54	2.53	3.36
	300	150	2700	Non-anch.	N/A	N/A	45	2.22	1.5	1.87	3.61	2.18	3.4
(Zhang, Elsayed, et al. 2021)	290	90	2100	anchorage	21.3	388	41	1.9	1.4	1.38	2.02	1.58	3.04
	290	90	2100	anchorage	42.7	365	41	1.9	1.4	1.04	2.13	1.55	2.63
	290	90	2100	anchorage	21.3	365	41	1.9	1.4	1.04	2.36	1.79	3.61
	290	90	2100	anchorage	21.3	388	41	1.9	1.4	1.38	3.87	3.18	6.81
	290	90	2100	anchorage	42.7	365	41	1.9	1.4	1.04	4.68	3.56	6.39
	290	90	2100	anchorage	21.3	365	41	1.9	1.4	1.04	4.47	3.43	7.06
	290	90	2100	anchorage	21.3	365	132	1.4	1.4	1.24	1.54	1.3	1.93
	290	90	2100	Non-anch.	21.3	365	41	1.9	1.4	1.04	1.03	1.02	0.99
	290	90	2100	anchorage	21.3	365	41	1.9	1.4	1.09	1.78	1.34	1.96
	290	90	2100	anchorage	21.3	365	41	1.9	1.4	1	2.42	1.9	3.65
(Wu et al. 2014)	300	150	2000	Non-anch.	34.4	340	170	1.55	1.3	1.24	3	2.26	4.02
	300	150	2000	Non-anch.	34.4	340	170	1.55	1.3	1.35	1.88	1.59	1.9
	300	150	2000	anchorage	34.4	340	170	1.55	1.3	1.35	3.23	2.41	3.44
(Ke et al. 2023)	300	150	3200	Non-anch.	47.6	502	151	1.32	1	0.88	1.45	1.4	1.37
	300	150	3200	anchorage	47.6	502	151	1.32	1	0.88	1.69	1.53	1.73
	300	150	3200	anchorage	48.9	502	151	1.32	1	0.88	1.93	1.71	1.82

	300	150	3200	anchorage	48.9	502	151	1.32	1	0.88	1.75	1.59	1.77
	300	150	3200	anchorage	48.7	502	151	1.32	1	0.88	1.65	1.46	1.78
	300	150	3200	anchorage	48.7	502	151	1.32	1	0.88	1.76	1.56	1.81
	300	150	3200	anchorage	49.2	502	151	1.32	1	0.88	1.82	1.55	1.87
	300	150	3200	anchorage	49.2	502	151	1.32	1	0.88	1.8	1.52	1.92
(Zhang, Ke, et al. 2021)	300	150	3200	Non-anch.	47.6	502	152	1.38	1	0.88	1.45	1.4	1.37
	300	150	3200	anchorage	47.6	502	152	1.38	1	0.88	1.8	1.63	1.79
	300	150	3200	Non-anch.	48.9	502	152	1.38	1	0.88	1.49	1.41	1.37
	300	150	3200	anchorage	48.9	502	152	1.38	1	0.88	1.7	1.53	1.65
	300	150	3200	anchorage	48.9	502	152	1.38	1	0.88	1.78	1.57	1.81
	300	150	3200	anchorage	48.9	502	152	1.38	1	0.88	1.85	1.65	1.71
	300	150	3200	anchorage	48.7	502	152	1.38	1	0.88	1.85	1.64	1.89
	300	150	3200	anchorage	48.7	502	152	1.38	1	0.88	2.08	1.75	2.17
	300	150	3200	anchorage	48.7	502	152	1.38	1	0.88	1.96	1.64	2.28
	300	150	3200	anchorage	48.7	502	152	1.38	1	0.88	2	1.62	2.31
(Saeed et al. 2018)	260	140	2700	Non-anch.	32.8	550	205	1.3	0.9	1.32	2	1.77	2.06
	260	140	2700	Non-anch.	32.8	550	212	1.4	0.9	1.34	1.57	1.48	2.56
	260	140	2700	Non-anch.	32.8	550	161	1.26	0.9	1.27	1.2	1.14	1.23
(Jung et al. 2017)	300	200	3400	Non-anch.	31.3	481	100	1.5	0.8	0.45	3.37	2.59	3.66
	300	200	3400	Non-anch.	31.3	481	167	1.48	0.8	0.45	3.12	2.49	3.44
	300	200	3400	Non-anch.	31.3	481	167	1.48	0.8	0.47	2.58	2.07	2.91
	300	200	3400	Non-anch.	31.3	481	121	1.55	0.8	0.49	2.14	1.72	2.17
	300	200	3400	Non-anch.	31.3	481	167	1.48	0.8	0.52	1.98	1.59	2.12
	300	200	3400	Non-anch.	31.3	481	167	1.48	0.8	0.52	2	1.6	2.45
	300	200	3400	Non-anch.	31.3	481	121	1.55	0.8	0.56	1.95	1.6	2.02
	300	200	3400	Non-anch.	31.3	481	121	1.55	0.8	0.56	1.88	1.42	1.89
(Zeng et al. 2021)	300	150	2000	Non-anch.	45.2	N/A	240	1.48	0.8	0.96	2.51	1.93	2.95
	300	150	2000	Non-anch.	45.2	N/A	179	1.51	0.8	0.99	2.15	1.68	2.37
(Obaidat, Barham, and Aljarah 2020)	250	200	1600	Non-anch.	35.3	N/A	170	1.7	0.8	0.76	1.57	1.45	1.98
	250	200	1600	Non-anch.	35.3	N/A	170	1.7	0.8	0.76	1.57	1.49	1.95
	250	200	1600	anchorage	35.3	N/A	170	1.7	0.8	0.76	3.01	2.61	4.37
	250	200	1600	Non-anch.	35.3	N/A	170	1.7	0.8	0.83	1.17	1.12	1.27
	250	200	1600	Non-anch.	35.3	N/A	170	1.7	0.8	0.83	1.18	1.14	1.18
	250	200	1600	anchorage	35.3	N/A	170	1.7	0.8	0.83	3.08	2.42	4.79
	250	200	1600	Non-anch.	35.3	N/A	170	1.7	0.8	0.9	1.24	1.19	1.4
	250	200	1600	Non-anch.	35.3	N/A	170	1.7	0.8	0.9	1.17	1.15	1.24
	250	200	1600	anchorage	35.3	N/A	170	1.7	0.8	0.9	2.96	2.17	4.59
(Tahmouresi, Momeninejad, and Mohseni 2022)	200	125	1500	Non-anch.	26	450	43	2.09	0.8	0.93	1.52	1.31	2.09
	200	125	1500	anchorage	26	450	43	2.09	0.8	0.93	2.69	1.93	3.47
	200	125	1500	anchorage	26	450	43	2.09	0.8	0.93	2.55	2.21	3.4
	200	125	1500	anchorage	26	450	43	2.09	0.8	0.93	1.82	1.64	2.39
	200	125	1500	anchorage	26	450	43	2.09	0.8	0.93	2.18	1.75	3.07
	200	125	1500	anchorage	26	450	43	2.09	0.8	0.93	2.3	2.04	3.16
(Boutlikht et al. 2022)	170	100	1000	Non-anch.	35	500	165	N/A	0.6	1.65	1.22	1.18	1.18
	170	100	1000	Non-anch.	35	500	165	N/A	0.6	1.65	1.73	1.75	1.8
	170	100	1000	Non-anch.	35	500	165	N/A	0.6	1.65	1.42	1.25	1.75
	170	100	1000	Non-anch.	35	500	165	N/A	0.6	1.65	1.81	1.52	1.6
(El-Gamal et al. 2016)	300	200	2700	Non-anch.	49.6	480	119	1.33	0.5	0.52	2.06	1.79	1.73
	300	200	2700	Non-anch.	49.6	480	119	1.33	0.5	0.61	1.84	1.52	1.78
	300	200	2700	Non-anch.	49.6	480	52	2.26	0.5	0.47	6.15	4.2	4.89
	300	200	2700	Non-anch.	49.6	480	52	2.26	0.5	0.51	3.82	2.67	3.46
	300	200	2700	Non-anch.	49.6	480	119	1.33	0.5	0.81	1.87	1.63	1.73
	300	200	2700	Non-anch.	49.6	480	52	2.26	0.5	0.76	1.98	1.72	1.74
	300	200	2700	Non-anch.	49.6	480	52	1.33	0.5	0.95	2.25	1.91	2.56
	300	200	2700	Non-anch.	49.6	480	52	1.33	0.5	1.04	1.61	1.46	1.68
(Xing, Chang, and Ozbulut 2018)	350	200	2100	Non-anch.	49.2	505	40	1.9	0.5	1.08	2.33	1.6	2.69
	350	200	2100	Non-anch.	46.8	498	40	1.9	0.5	0.72	2.46	1.64	2.83
	350	200	2100	Non-anch.	47.3	498	40	1.9	0.5	0.77	2.16	1.48	2.44
(Darain et al. 2016)	250	125	3300	Non-anch.	50.1	529	165	1.6	0.5	1.04	1.98	1.64	2.21
	250	125	3300	Non-anch.	50.1	529	165	1.6	0.5	1.12	1.54	1.34	1.63
	250	125	3300	Non-anch.	50.1	529	165	1.6	0.5	1.12	1.9	1.54	1.89
	250	125	3300	Non-anch.	50.1	529	165	1.6	0.5	1.21	1.57	1.41	1.6
	250	125	3300	Non-anch.	50.1	529	165	1.6	0.5	1.38	1.52	1.35	1.71
(Hadi 2022)	300	250	4000	Non-anch.	21	400	225	1.9	0.4	0.82	2.72	2.48	4.15
	300	250	4000	Non-anch.	21	400	155	1.8	0.4	0.77	3.02	2.74	4.79
	300	250	4000	Non-anch.	21	400	225	1.9	0.4	0.83	2.48	2.27	3.99
	300	250	4000	Non-anch.	21	400	225	1.9	0.4	0.86	3.54	3.2	5.19
(Imjai et al. 2023)	250	150	2500	Non-anch.	15.3	392	120	1.5	0.4	0.81	2.34	2.04	2.48
	250	150	2500	Non-anch.	15.3	392	120	1.5	0.4	0.91	2.05	1.74	2.28
(Abdallah et al. 2020)	280	150	3000	Non-anch.	37	600	146	1.3	0.3	0.71	2.17	1.85	3.33
	280	150	3000	Non-anch.	37	600	146	1.3	0.3	0.71	1.25	1.19	1.5
	280	150	3000	Non-anch.	37	600	146	1.3	0.3	0.71	1.64	1.44	2.27
	280	150	3000	Non-anch.	37	600	146	1.3	0.3	0.71	0.99	0.99	0.99
	280	150	3000	Non-anch.	37	600	146	1.3	0.3	0.71	2.1	1.84	3.2
(Dias, Barros, and Janwaen 2018)	300	150	2600	Non-anch.	50.2	567	175	1.8	0.3	0.41	3.24	2.52	4.5
	300	150	2600	Non-anch.	50.2	567	175	1.8	0.3	0.44	2.68	1.99	3.54
	300	150	2600	Non-anch.	50.2	567	175	1.8	0.3	0.47	2.27	1.71	2.84
(Nurbaiah et al. 2010)	250	150	2325	Non-anch.	N/A	N/A	40	1.9	0.3	0.75	5.06	3.44	5.03
	250	150	2325	Non-anch.	N/A	N/A	40	1.9	0.3	0.82	2.66	2.09	2.35

*: non anchorage; **: anchorage; N/A: Not applicable

2.3 Statistical Examination

Multivariate analysis of variance (MANOVA) is an expansion of the univariate technique known as ANOVA. It is a statistical procedure that allows for the simultaneous examination of data with multiple dependent variables. MANOVA aims to explore the correlation between a set of dependent measures and groups formed by one or more categorical independent measures. In this study, we employed MANOVA to examine the differences in mean values for ductility indices (μ_N, μ_p, and μ_o) across various TESR% groups, which served as our categorical independent variable. Before proceeding with data analysis, we ensured that several assumptions required for a MANOVA were met. These included assessing normality, linearity, equality of variance matrices, and identifying any multivariate outliers. MANOVA was chosen for analyzing the data related to the first research question because it allows for examining group differences (independent variables) in linear combinations of quantitative dependent variables. By using MANOVA, we were able to identify mean differences in the evaluation of three types of ductility indices between the TESR% group (Tabachnick 2019).

Following a non-significant result in the MANOVA, a post hoc Multivariate Analysis of Covariance (MANCOVA) was performed. The purpose of this subsequent analysis is to determine if there are any significant variances among independent groups concerning multiple continuous dependent variables while accounting for the influence of one or more covariates. It is important to note that several assumptions must be met for a standard MANCOVA analysis to be considered valid. Moreover, the Johnson-Neyman technique offers a robust alternative to ANCOVA in experimental designs when there is a violation of the assumption of homogeneity of regression slopes. This method provides researchers with valuable insights into the precise area where independent effects are not statistically significant. To simplify, the Johnson-Neyman approach is utilized to showcase the moderating effect in a simple slope analysis. Recently, there has been a growing interest in the implementation of the Johnson-Neyman technique, which has been adjusted to handle cases involving continuous moderators. The analysis involved using 10,000 bootstrap samples and reporting the effects with bias-corrected 95% confidence intervals.

3. Statistical Test Results

3.1 MANOVA test results

To ensure the validity of MANOVA, it is crucial to examine various assumptions such as normality, linearity, homogeneity of covariance matrices, and the presence of multivariate outliers. To evaluate multivariate normality, Table 2 presents the results of a normality test for three variables: μ_N, μ_p, and μ_0 (ductility indices). The K-S test indicates a non-normal data distribution for μ_N, μ_p, and μ_0 due to p-values <0.05. This non-normality could affect further statistical analyses, requiring alternative methods or transformations. In this study, a two-step transformation method introduced by Templeton (Templeton 2011) was utilized to normalize the ductility indices μ_{NN}, μ_{pN}, and μ_{0N}, as presented in Table 3.

Table 2. Tests of normality

Ductility Indices	TESR%	Kolmogorov-Smirnov			Shapiro-Wilk		
		Statistic	df	Sig.	Statistic	df	Sig.
μ_{NN}	<= 0.755	0.188	25	0.023	0.866	25	0.004
	0.756 - 0.885	0.269	30	0	0.7	30	0
	0.886 - 1.038	0.126	19	0.200*	0.969	19	0.761
	1.039+	0.182	24	0.038	0.892	24	0.015
μ_{PN}	<= 0.755	0.21	25	0.006	0.858	25	0.003
	0.756 - 0.885	0.264	30	0	0.828	30	0
	0.886 - 1.038	0.179	19	0.111	0.861	19	0.01
	1.039+	0.219	24	0.004	0.876	24	0.007
μ_{0N}	<= 0.755	0.137	25	0.200*	0.951	25	0.261
	0.756 - 0.885	0.264	30	0	0.741	30	0
	0.886 - 1.038	0.184	19	0.09	0.878	19	0.02
	1.039+	0.203	24	0.011	0.776	24	0

*: This is a lower bound of the true significance

Table 3. Tests of normality after two step transforms

Ductility Indices	TESR%	Kolmogorov-Smirnov			Shapiro-Wilk		
		Statistic	df	Sig.	Statistic	df	Sig.
μ_{NN}	<= 0.755	0.055	25	0.200*	0.974	25	0.752
	0.756 - 0.885	0.047	30	0.200*	0.979	30	0.789
	0.886 - 1.038	0.064	19	0.200*	0.993	19	1
	1.039+	0.058	24	0.200*	0.973	24	0.736
μ_{PN}	<= 0.755	0.055	25	0.200*	0.974	25	0.752
	0.756 - 0.885	0.046	30	0.200*	0.979	30	0.807
	0.886 - 1.038	0.04	19	0.200*	0.993	19	1
	1.039+	0.058	24	0.200*	0.973	24	0.736
μ_{0N}	<= 0.755	0.055	25	0.200*	0.974	25	0.752
	0.756 - 0.885	0.046	30	0.200*	0.979	30	0.807
	0.886 - 1.038	0.081	19	0.200*	0.946	19	0.335
	1.039+	0.058	24	0.200*	0.973	24	0.736

*: This is a lower bound of the true significance

Table 4. Mahalanobis distance test

	Residuals Statistics				
	Min.	Max.	Mean	Std. Deviation	N
Std. Predicted value	-2.733-	2.372	0	1	98
Standard error of predicted value	0.122	0.455	0.218	0.074	98
Adjusted predicted value	2.22	2.76	2.43	0.067	98
Residual	-1.477-	1.613	0	1.121	98
Std. Residual	-1.296-	1.416	0	0.984	98
Stud. Residual	-1.414-	1.471	-0.001-	1.006	98
Deleted residual	-1.756-	1.779	-0.002-	1.172	98
Stud. Deleted residual	-1.421-	1.48	0	1.01	98
Mahal. Distance	0.123	14.51	2.969	2.973	98
Cook's distance	0	0.095	0.012	0.016	98
Centered leverage value	0.001	0.15	0.031	0.031	98

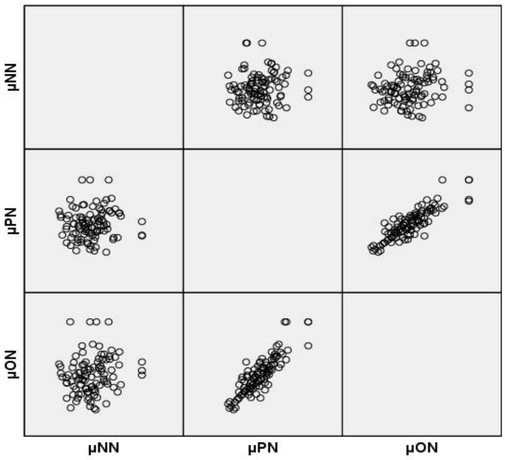

Fig. 4 Scatterplot matrix

The hypothesis of linearity suggests that there should be a linear relationship between each dependent variable and another. To validate this assumption, a scatterplot matrix is often employed to reveal their relationships. In Fig. 4, we can observe a graphical representation of a linear relationship among the dependent variables, thereby indicating acceptance of the Linearity hypothesis. Moreover, the presence of multivariate outliers was the crucial assumption investigated in the analysis of MANOVA. To identify any potential outliers, a multiple linear regression was conducted on the dependent variables (ductility indices). Subsequently, a Mahalanobis variable was generated and sorted in descending order. To determine if an observation is an outlier, it is necessary to know the critical chi-square value. This specific value was determined at p = 0.001. where the degrees of freedom (df) correspond to the number of dependent variables. The present study had three degrees of freedom for the multivariate analysis of variance (MANOVA). The critical value of 16.27 was determined at a significant level of p = 0.001. Accordingly, any observation with a Mahalanobis Distance greater than 16.27 should be considered for removal based on the findings. The maximum recorded Mahalanobis Distance for MANOVA in Table 4 of the Residual Statistics was only 14.51, indicating that no outliers were identified during the analysis. This result confirms that there are no outliers present, as required by the MANOVA analysis. In addition, the null hypothesis was examined based on the assumption that the observed variance matrices of the dependent variables are similar across groups. To verify this hypothesis, a Box's M test was performed. Unlike many other tests, this test, as shown in Table 5, is known for its strictness, with the level of significance typically set at 0.001.

Table 5. Box's Test of Equality of Covariance Matrices

Box's M	7.807
F	0.408
df1	18
df2	25110.485
Sig.	0.987

The resulting p-value from the test revealed a significant value of 0.987, suggesting that there is sufficient evidence to indicate that the assumption of homogeneity of covariance among the dependent variables has been met for the groups defined by the categorical independent factor. Therefore, it was deemed appropriate to proceed with the MANOVA analysis. As indicated by the Tests of Between-Subjects Effects presented in Table 6, the results from the MANOVA revealed that there were no statistically significant differences observed in the ductility indices μ_{NN}, μ_{pN}, and μ_{0N} within the TESR% group. Thus, a post hoc analysis utilizing MANCOVA was implemented to account for covariate variables (i.e., stirrup ratio ρsv% and presence of anchorage) while analyzing differences among ductility indices within the TESR% group.

Table 6. MANOVA test results

Source	Dependent variable	Tests of between-subjects effects					
		type III sum of squares	df	Mean square	F	Sig.	Partial eta squared
Corrected model	μ_{NN}	0.182	3	0.061	0.068	0.977	0.002
	μ_{pN}	0.076	3	0.025	0.068	0.977	0.002
	μ_{0N}	0.056	3	0.019	0.01	0.999	0
Intercept	μ_{NN}	518.103	1	518.103	582.06	0	0.861
	μ_{pN}	336.355	1	336.355	909.402	0	0.906
	μ_{0N}	723.531	1	723.531	405.355	0	0.812
TESR%	μ_{NN}	0.182	3	0.061	0.068	0.977	0.002
	μ_{pN}	0.076	3	0.025	0.068	0.977	0.002
	μ_{0N}	0.056	3	0.019	0.01	0.999	0
Error	μ_{NN}	83.671	94	0.89			
	μ_{pN}	34.767	94	0.37			
	μ_{0N}	167.784	94	1.785			
Total	μ_{NN}	618.208	98				
	μ_{pN}	381.435	98				
	μ_{0N}	911.728	98				
Corrected total	μ_{NN}	83.853	97				
	μ_{pN}	34.843	97				
	μ_{0N}	167.84	97				

3.2 MANCOVA test results

Table 7. MANCOVA test with covariate variable results

Source	Dependent variable	Tests of between-subjects effects					
		type III sum of squares	df	Mean square	F	Sig.	Partial eta squared
TESR% × ρ_{sv}%	μ_{NN}	8.317	3	2.772	3.379	0.022	0.105
	μ_{pN}	9.085	3	3.028	11.29	0	0.283
	μ_{0N}	41.462	3	13.821	11.965	0	0.294
TESR %× anchorage	μ_{NN}	0.492	3	0.164	0.2	0.896	0.007
	μ_{pN}	1.835	3	0.612	2.281	0.085	0.074
	μ_{0N}	4.234	3	1.411	1.222	0.307	0.041
Error	μ_{NN}	70.553	86	0.82			
	μ_{pN}	23.067	86	0.268			
	μ_{0N}	99.34	86	1.155			
Total	μ_{NN}	618.21	98				
	μ_{pN}	381.44	98				
	μ_{0N}	911.73	98				
Corrected total	μ_{NN}	83.853	97				
	μ_{pN}	34.843	97				
	μ_{0N}	167.84	97				

In addition to the longitudinal reinforcement ratio, there are multiple parameters that interact with each other and influence the ductility at ultimate limit states. Earlier studies have demonstrated that when concrete is confined through appropriate arrangements of transverse reinforcement (stirrup), it leads to a significant enhancement in both the strength and ductility of the structural element. To investigate the impact of the interaction parameters on the ductility of beams, MANCOVA was used as a post hoc analysis to control for covariate variables (stirrup ratio) and existing anchorage and assess the differences in ductility indices within the TESR% group. Utilizing MANCOVA as a post hoc analysis necessitates the validation of various assumptions before performing the analysis. These assumptions include the absence of outliers, normality, linearity, and homogeneity of covariance. It is worth mentioning that all of these assumptions were already checked during the MANOVA analysis and found to be met except for homogeneity of covariance. The homogeneity of regression plays a central role in group analyses that involve covariates, such as ANCOVA and MANCOVA. This assumption asserts that the slopes of the regression lines for each covariate are uniform across the independent variable group [27]. To evaluate whether this assumption is valid, a MANCOVA model can be implemented in SPSS. In the model options, it is crucial to include interactions between the covariates and the independent variable. If there is a significant interaction p<0.05, it indicates a violation of the homogeneity assumption regarding regression coefficients. Referring to Table 7, where interactions are displayed between the stirrup ratio as covariates and TESR% as an independent variable, the results of the p-value revealed the violation of the assumption of homogeneity of regression. Consequently, we cannot proceed with implementing and interpreting our MANCOVA due to this violation.

3.3 Johnson-Neyman method test results

To address the violation of homogeneity of regression, we conducted an analysis using the Johnson-Neyman method in the process software program for SPSS. This method was employed to investigate the moderating influence of the stirrup ratio on the association between the TESR variable and the ductility index variables. A moderating variable can be qualitative or quantitative and influences the strength or direction of the relationship between an independent variable and a dependent variable. To establish a variable as a moderating variable, there must be a statistically significant interaction between the independent and the moderator (p <0.05). We investigated this interaction at various values of the moderator to determine the point at which the effect of TESR% on ductility indices became significant. Table 8 presents the moderator analyses. As anticipated, we observed a significant interaction between the stirrup ratio moderation and TESR% in predicting ductility indices, μ_{NN} (B=-2.2785, P=0.0005<0.05), μ_{PN} (B=2.0434, P=0.0000<0.05), μ_{0N} (B= 4.4087, P=0.0000<0.05).

According to Fig. 5a, there is a positive correlation between the TESR% and the Naaman and Jeong index (μ_{NN}) for the high stirrup ratio. When looking at both mean and low values of the stirrup ratio, there is a negative effect between TESR% and the Naaman and Jeong index (μ_{NN}). Similarly, as depicted in Fig. 5b and 5c, we observe the same relationship between the TESR% and the ductility indices, the Davies index (μ_{PN}) and the Oudah and El-Hacha index (μ_{0N}). Except a steeper slope was observed for the relationship between the TESR% and the Oudah and El-Hacha index (μ_{0N}), regardless of whether the stirrup ratio was high or low. In terms of the ductility index value, the Oudah and El-Hacha index (μ_{0N}) have greater values than the other two ductility indices. This can be attributed to the fact that the calculation for the Oudah and El-Hacha index (μ_{0N}) relies on the deformability ratio, making it greater than others. This result is consistent with the conclusion stated by (Jen Hua Ling, Yong Tat Lim, and Euniza Jusli 2023). To further examine the effect of moderation, we utilized the Johnson-Neyman method. This method allowed us to assess interactions and identify areas where statistical significance was present, along with their respective thresholds. A confidence level of 95% and an alpha level of 0.05 were employed in the Johnson-Neyman.

Fig.6 displays the regions of statistical significance according to the Johnson-Neyman method for the impact of TESR% on the Naaman and Jeong index (μ_{NN}). These regions are based on different levels of stirrup ratio ρ_{SV}% acting as moderator. The results show that when the stirrup ratio is at or below -0.1779 (which corresponds to an actual value of 0.74%), it indicates that there are ranges where TESR% has a statistically significant negative effect on the Naaman and Jeong index (μ_{NN}). Conversely, if we consider values between -0.1779 and 0.5646 (equivalent to stirrup ratio ranging from 0.74% to 1%), there doesn't appear to be any association between TESR% and the Naaman and Jeong index (μ_{NN}) within this particular range. The same figure shows a significant effect of TESR% on the Naaman and Jeong index (μ_{NN}) in RC beams strengthened with the FRP-NSM system within the region where the stirrup ratio is at or above 0.5646 (which corresponds to an actual value of 1%). As indicated by the Naaman and Jeong index (μ_{NN}), the effect of TESR% on the ductility index consists of a broad range of insignificant regions. This is because the additional elastic energy of the post-yielding stage is ignored in the index calculation of reinforced concrete beams reinforced with FRP materials. As a result, these findings have the potential to provide misleading values when evaluating ductility. Therefore, according to Oudah and El-Hacha's recommendations accurately assessing RC beams strengthened with FRP materials cannot be accomplished using the Naaman and Jeong index (μ_{NN}).

Table 8. TESR%, stirrup ratio psv%, and their interaction as predictors of ductility Indice

Independent variables	Naaman and Jeong idex μ_{NN}		Davies index μ_{PN}		Oudah and El-Hacha idex μ_{0N}	
	B (SE)	Sig	B (SE)	Sig	B (SE)	Sig
TESR%	-0.3084 (0.3445)	0.9717	0.0265 (0.197)	0.8932	-0.1556 (0.4236)	0.7142
ρ_{SV}%	-0.1785 (0.6503)	0.6757	-0.6384 (0.2383)	0.0087	-1.0377 (0.5123)	0.0457
TESR%× ρ_{SV}%	2.2785 (0.0019)	0.0005	2.0434 (0.4328)	0	4.4087 (0.9303)	0
*Anchorage	-0.0166 (0.9469)	0.489	0.4858 (0.1506)	0.0017	1.2641 (0.3238)	0.0002

*Anchorage: a covariate variable

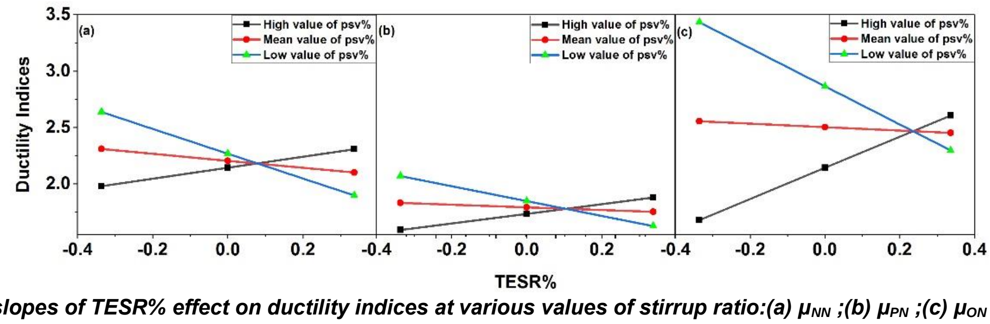

Fig. 5 The simple slopes of TESR% effect on ductility indices at various values of stirrup ratio:(a) μ_{NN} ;(b) μ_{PN} ;(c) μ_{ON}

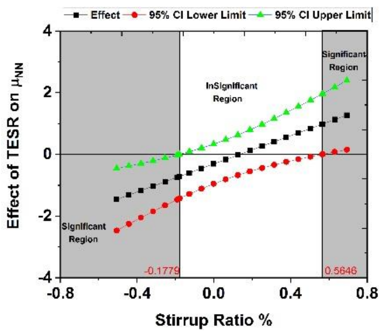

Fig. 6 The Johnson-Neyman graph displaying interaction effect of TESR% and stirrup ratio on the Naaman and Jeong index (μ_{NN})

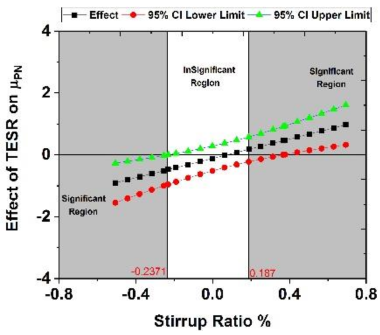

Fig. 7 The Johnson-Neyman graph displaying interaction effect of TESR% and stirrup ratio on the Davies index (μ_{PN})

In contrast, Fig. 7 of the Johnson-Neyman method illustrates how a moderator (stirrup ratio ρ_{SV}%) can influence and shape the relationship between TESR% and the Davies index (μ_{PN}). The findings indicate that when the stirrup ratio falls at or below -0.2371 (0.72% in real terms), there is a considerable negative impact of TESR% on the Davies index (μ_{PN}). On the other hand, for cases where the stirrup ratio ranges from 0.1870 to -0.2371 (0.72% to 0.87% in real terms), an insignificant effect of TESR% on the Davies index (μ_{PN}) was observed. Additionally, an interesting discovery was made showing that when the stirrup ratio reaches 0.1870 (0.87% in real terms) and beyond, TESR% plays a critical positive role in enhancing the Davies index (μ_{PN}). The results from this study reveal a wide spectrum of substantial influence of the TESR% on the Davies index (μ_{PN}), Specifically, there is a substantial negative influence indicated by an approximately 30% shaded area, as well as a noticeable positive effect depicted by another shaded area covering roughly 50%. Consequently, the revised method yields a greater area of outcomes when estimating the ductility index compared to the Naaman and Jeong index (μ_{NN}). This enhancement occurs by considering the additional elastic energy produced within any Fiber reinforced polymer (FRP) strengthened RC beams during the last stages of loading.

Similarly, Fig. 8 of the Johnson-Neyman method depicts regions of significance for the moderated effects of TESR% on the Oudah and El-Hacha index (μ_{0N}). If the stirrup ratio is less than -0.1756 (0.74% in real terms), then the effect of TESR on the Oudah and El-Hacha index (μ_{0N}) decreases significantly. In cases where the stirrup ratio is between -0.1756 to 0.2429 (0.74% to 0.89% in real terms), there is no notable effect observed of the TESR% on the Oudah and El-Hacha index (μ_{0N}). However, if the stirrup ratio is equal to or exceeds 0.2429 (0.89% in real terms), there will be a positive increase in the impact of TESR% on the Oudah and El-Hacha index (μ_{0N}). It is important to highlight that, when compared to the Naaman and Jeong index (μ_{NN}), the findings indicate a wider range of significant regions in terms of the influence of TESR% on the Oudah and El-Hacha index (μ_{0N}). This could be attributed to characteristics inherent in a ductility model developed based on the response of a typical steel RC beam strengthened using FRP material.

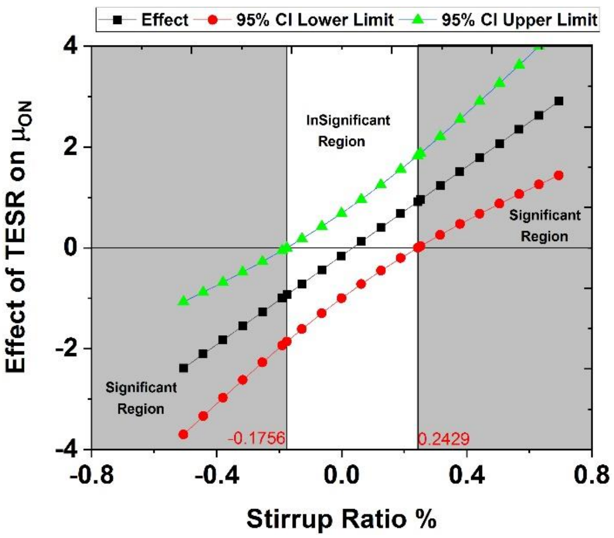

Fig. 8 The Johnson-Neyman graph displaying interaction effect of TESR% and Stirrup Ratio on the Oudah and El-Hacha index μ_{ON}

4. Conclusions

In summary, this study explored the efficiency and limitations of energy-based ductility indices of RC beams strengthened with FRP materials. The objective was to overcome the existing knowledge gap on which ductility indices are more appropriate to use in assessing the performance of such beams. A statistically robust approach was employed to determine the efficacy of different energy-based ductility indices. In this analysis, the influence of TESR% on the calculated ductility index values was taken into account.

Based on the obtained results, the following aspects can be concluded:

1. The MANOVA results demonstrate no significant variance in the three ductility index measurements μ_{NN}, μ_{PN}, and μ_{0N} among the TESR% group because the ductility of the RC beams strengthened with FRP materials is impacted by various parameters that interact with TESR% and cause an effect.
2. The MANCOVA test indicated an interaction between the stirrup ratio and TESR%, which affects the ductility indices. This interaction was observed because the assumption of homogeneity of regression slopes was violated. According to this assumption, the regression slopes for covariates should be consistent across groups. The presence of an interaction effect suggests that the influence of the independent variable (TESR%) is not the same across different levels of the covariate (stirrup ratio ρ_{SV}%.).
3. Based on the data from the Johnson-Neyman method, an interesting observation is made about the correlation between TESR% and ductility indices. The impact of this relationship varies depending on different levels of stirrup ratio ρ_{SV}%, resulting in negative, positive, or insignificant effects within specific ranges. Notably, a wide range of negligible impacts for TESR% on The Naaman and Jeong index (μ_{NN}) was shown, varying from 0.74% to 1% in reinforced concrete beams strengthened with FRP materials. This result is because the post-yielding stages of reinforced concrete beams that were strengthened with FRP materials were not taken into account. Consequently, these outcomes can potentially produce misleading values for assessing ductility.
4. On the other hand, when examining the Davies index (μ_{PN}) and the Oudah and El-Hacha Idex (μ_{0N}), it becomes evident that they reveal a limited range of negligible effects on ductility indices when subjected to varying levels of stirrup ratio ρ_{SV}%. The threshold for μ_{PN} ranges between 0.72% to 0.87%, while for μON it ranges from 0.74% to 0.89%. It is worth noting that the large region of the impact of TESR% on the Davies index (μ_{PN}) and the Oudah and El-Hacha Idex (μ_{0N}) was demonstrated, which gives a powerful basis for these methods in ductility assessment.
5. The Oudah and El-Hacha index (μ_{0N}) have higher values than the other ductility indices as a result of taking the deformability ratio into account when calculating them, which explains this distinction. The Davies index (μ_{PN}), in contrast, typically had lower values than the other two ductility measures, making it more conservative.

Conflicts of Interest

The authors declare no conflict of interest

References

Abdallah, Mohammad, Firas Al Mahmoud, Rémi Boissiere, Abdelouahab Khelil, and Julien Mercier. 2020. 'Experimental study on strengthening of RC beams with Side Near Surface Mounted technique-CFRP bars', Composite Structures, 234: 111716. https://doi.org/10.1016/j.compstruct.2019.111716

Boutlikht, Mourad, Noureddine Lahbari, Seifeddine Tabchouche, and Kamel Hebbache. 2022. 'Behavior of strengthened reinforced concrete beams under different CFRP strips arrangement', Innovative Infrastructure Solutions, 7: 206. https://doi.org/10.1007/s41062-022-00811-1

Darain, Kh Mahfuz Ud, Mohd Zamin Jumaat, Ahmad Azim Shukri, M Obaydullah, Md Nazmul Huda, Md Akter Hosen, and Nusrat Hoque. 2016. 'Strengthening of RC beams using externally bonded reinforcement combined with near-surface mounted technique', Polymers, 8: 261. https://doi.org/10.3390/polym8070261

Davies, Paul. 2010. 'Ductility and deformability of FRP strengthened reinforced concrete structures', University of South Wales (United Kingdom).

Dias, Salvador JE, Joaquim AO Barros, and Worajak Janwaen. 2018. 'Behavior of RC beams flexurally strengthened with NSM CFRP laminates', Composite Structures, 201: 363-76. https://doi.org/10.1016/j.compstruct.2018.05.126

El-Gamal, S EI, A Al-Nuaimi, A Al-Saidy, and A Al-Lawati. 2016. 'Efficiency of near surface mounted technique using fiber reinforced polymers for the flexural strengthening of RC beams', Construction and Building Materials, 118: 52-62. https://doi.org/10.1016/j.conbuildmat.2016.04.152

El-Hacha, Raafat, and Sami H Rizkalla. 2004. 'Near-surface-mounted fiber-reinforced polymer reinforcements for flexural strengthening of concrete structures', Structural Journal, 101: 717-26. https://doi.org/10.14359/13394

Hadi, Saheb. 2022. "Full-scale experimental evaluation of flexural strength and ductility of reinforced concrete beams strengthened with various FRP mechanisms." In Structures, 1160-76. Elsevier. https://doi.org/10.1016/j.istruc.2022.07.011

Imjai, Thanongsak, Monthian Setkit, Fabio P Figueiredo, Reyes Garcia, Worathep Sae-Long, and Suchart Limkatanyu. 2023. 'Experimental and numerical investigation on low-strength RC beams strengthened with side or bottom near surface mounted FRP rods', Structure and Infrastructure Engineering, 19: 1600-15. https://doi.org/10.1080/15732479.2022.2045613

Jen Hua Ling, Dr Ir, Mr Yong Tat Lim, and Mdm Euniza Jusli. 2023. "Methods to determine ductility of structural members: a review." In Journal of the Civil Engineering Forum, 181-94. Universitas Gadjah Mada.

Jung, Woo-tai, Jong-sup Park, Jae-yoon Kang, and Moon-seoung Keum. 2017. 'Flexural behavior of concrete beam strengthened by near-surface mounted CFRP reinforcement using equivalent section model', Advances in Materials Science and Engineering, 2017. https://doi.org/10.1155/2017/9180624

Ke, Y, SS Zhang, ST Smith, and T Yu. 2023. 'Novel Embedded FRP Anchor for RC Beams Strengthened in Flexure with NSM FRP Bars: Concept and Behavior', Journal of Composites for Construction, 27: 04022093. https://doi.org/10.1061/(ASCE)CC.1943-5614.000127

Mufti, Aftab A, John P Newhook, and G Tadros. 1996. "Deformability versus ductility in concrete beams with FRP reinforcement." In PROCEEDINGS OF THE 2ND INTERNATIONAL CONFERENCE ON ADVANCED COMPOSITE MATERIALS IN BRIDGES AND STRUCTURES, ACMBS-II, MONTREAL 1996.

Naaman, A, and M Jeong. 1995. "45 Structural ductility of concrete beams prestressed with FRP tendons." In Non-Metallic (FRP) Reinforcement for concrete structures: proceedings of the second international RILEM symposium, 379. CRC Press Boca Raton, FL, USA.

Nurbaiah, MN, AH Hanizah, A Nursafarina, and M Nur Ashikin. 2010. "Flexural behaviour of RC beams strengthened with externally bonded (EB) FRP sheets or Near Surface Mounted (NSM) FRP rods method." In 2010 International Conference on Science and Social Research (CSSR 2010), 1232-37. IEEE.

Obaidat, Yasmeen Taleb, Wasim S Barham, and Abdelmalek H Aljarah. 2020. 'New anchorage technique for NSM-CFRP flexural strengthened RC beam using steel clamped end plate', Construction and Building Materials, 263: 120246. https://doi.org/10.1016/j.conbuildmat.2020.120246

Oudah, Fadi, and Raafat El-Hacha. 2012. 'A new ductility model of reinforced concrete beams strengthened using fiber reinforced polymer reinforcement', Composites Part B: Engineering, 43: 3338-47. https://doi.org/10.1016/j.compositesb.2012.01.071

Saeed, Ikram A, Riadh Al-Mahaidi, Tareq S Al-Attar, and Basil S Al-Shathr. 2018. 'Flexural behavior of RC beams strengthened by NSM-CFRP laminates or bars', Engineering and Technology Journal, 36: 358-67. http://dx.doi.org/10.30684/etj.36.4A.1

Salahaldin, Ali I, Muyasser M Jomaa'h, and Dlovan M Naser. 2021. 'Flexural Behavior of Damaged Lightweight Reinforced Concrete Beams Strengthened by CFRP', Journal of Engineering Research, 9. https://doi.org/10.36909/jer.v9iICRIE.11647

Salahaldin, Ali I, Muyasser M Jomaa'h, Nazar A Oukaili, and Diyaree J Ghaidan. 2022. 'Rehabilitation of hybrid RC-I beams with openings using CFRP sheets', Civil Engineering Journal, 8: 155-66. http://dx.doi.org/10.28991/CEJ-2022-08-01-012

Spadea, Giuseppe, Francesco Bencardino, Fabio Sorrenti, and Ramnath Narayan Swamy. 2015. 'Structural effectiveness of FRP materials in strengthening RC beams', Engineering Structures, 99: 631-41. https://doi.org/10.1016/j.engstruct.2015.05.021

Tabachnick, BG. 2019. "Chapter 13 in Using Multivariate Statistics (ed. Tabachnick, BG, Fidell, LS) 476–527." In.: Allyn & Bacon/Pearson Education.

Tahmouresi, Behzad, Kasra Momeninejad, and Ehsan Mohseni. 2022. 'Flexural response of FRP-strengthened lightweight RC beams: hybrid bond efficiency of L-shape ribbed bars and NSM technique', Archives of Civil and Mechanical Engineering, 22: 95. https://doi.org/10.1007/s43452-022-00410-y

Templeton, Gary F. 2011. 'A two-step approach for transforming continuous variables to normal: implications and recommendations for IS research', Communications of the association for information systems, 28: 4.

Wu, Gang, Zhi-Qiang Dong, Zhi-Shen Wu, and Li-Wei Zhang. 2014. 'Performance and parametric analysis of flexural strengthening for RC beams with NSM-CFRP bars', Journal of Composites for Construction, 18: 04013051. https://doi.org/10.1061/(ASCE)CC.1943-5614.0000451

Xing, Guohua, Zhaoqun Chang, and Osman E Ozbulut. 2018. 'Behavior and failure modes of reinforced concrete beams strengthened with NSM GFRP or aluminum alloy bars', Structural Concrete, 19: 1023-35. https://doi.org/10.1002/suco.201700099

Zeng, Yihua, Xi Chen, Xinghua Li, and Gang Wu. 2021. 'Strengthening of RC beams using the combination of EB CFRP sheet, NSM CFRP bar and P-SWRs', Structural Concrete, 22: 132-45. https://doi.org/10.1002/suco.201900522

Zhang, SS, Y Ke, ST Smith, HP Zhu, and ZL Wang. 2021. 'Effect of FRP U-jackets on the behaviour of RC beams strengthened in flexure with NSM CFRP strips', Composite Structures, 256: 113095. https://doi.org/10.1016/j.compstruct.2020.113095

Zhang, Y, M Elsayed, LV Zhang, and ML Nehdi. 2021. 'Flexural behavior of reinforced concrete T-section beams strengthened by NSM FRP bars', Engineering Structures, 233: 111922. https://doi.org/10.1016/j.engstruct.2021.111922

Disclaimer